Sunitinib treatment exacerbates intratumoral heterogeneity in metastatic renal cancer

Authors: Grant D Stewart[1,2], Fiach C O'Mahony[1,2], Alexander Laird[1,2,3], Lel Eory[3,*], Alexander LR Lubbock[3], Alan Mackay[4], Jyoti Nanda[1,2], Marie O'Donnell[1,2], Peter Mullen[5], S Alan McNeill[1,2], Antony CP Riddick[1,2,†], Daniel Berney[6], Axel Bex[7], Michael Aitchison[2,8], Ian M Overton[3], David J Harrison[2,5], Thomas Powles[8,9]

Affiliations:

[1]Edinburgh Urological Cancer Group, Division of Pathology, Institute of Genetics and Molecular Medicine, University of Edinburgh, Edinburgh, EH4 2XU, UK.

[2]Scottish Collaboration On Translational Research into Renal Cell Cancer (SCOTRRCC).

[3]MRC Human Genetics Unit, Institute of Genetics and Molecular Medicine, University of Edinburgh, Edinburgh, EH4 2XU, UK.

[4]Divisions of Molecular Pathology and Cancer Therapeutics, The Institute of Cancer Research, 15 Cotswold Road, Belmont, Sutton, Surrey, SM2 5NG, UK.

[5]School of Medicine, University of St Andrews, KY16 9AJ, UK.

[6]Department of Molecular Oncology, Bart's Cancer Institute, London, EC1M 6BQ, UK.

[7]Department of Urology, Netherlands Cancer Institute, 1006 BE Amsterdam, The Netherlands.

[8]Renal Cancer Unit, The Royal Free Hospital, London, NW3 2QG, UK.

[9]Centre for Experimental Cancer Medicine, Bart's Cancer Institute, Queen Mary University of London, EC1A 7BE, UK.

[*] Current address: The Roslin Institute and R(D)SVS, University of Edinburgh, Easter Bush, Midlothian, EH25 9RG, UK

[†] Current address: Department of Urology, Addenbrooke's Hospital, Cambridge, CB2 0QQ, UK

Running title: Increased molecular heterogeneity following sunitinib

Keywords: Biomarker; Molecular; Heterogeneity; Renal cancer; VEGF TKI

Financial support: Chief Scientist Office, Scotland (ETM37; GDS, ACPR, MA, DJH), Cancer Research UK (Experimental Cancer Medicine Centre) (TP, London and DJH, Edinburgh), Medical Research Council (AL, DJH), Royal College of Surgeons of Edinburgh (AL), Melville Trust (AL), Medical Research Council (MC_UU_12018/25; IMO), Royal Society of Edinburgh Scottish Government Fellowship cofunded by Marie Curie Actions (IMO), Renal Cancer Research Fund (GDS), Kidney Cancer Scotland (GDS) and an educational grant from Pfizer (TP).

Corresponding author: Professor Thomas Powles, Head of Translational Oncology, Experimental Cancer Medicine Centre, Bart's Cancer Institute, Queen Mary University of London, London, EC1A 7BE. Fax +44 (0)207 6018522. Tel +44 (0)207 6018522. Email: thomas.powles@bartshealth.nhs.uk

Conflicts of interest: Axel Bex and Thomas Powles have participated on advisory boards for Pfizer and GSK for which they received financial compensation.

Translational relevance

The effect of targeted therapy on intratumoral heterogeneity has not been studied in renal cancer. We report a study using a unique set of sunitinib naïve and treated clear cell renal cancer samples from patients with metastatic disease enrolled in clinical trials. There was significant intratumoral heterogeneity at protein, mRNA and DNA levels. Following sunitinib therapy there was increased intratumor heterogeneity of tumor grade, renal cancer driver gene mutations (mRNA and DNA) and protein expression. Despite this, consistent genetic alterations to key renal cancer genes occurred following sunitinib therapy. These results suggest that the commonly proposed mechanism of drug treatment enforcing clonal selection of a pre-existing clone should be reconsidered. Instead it appears that the tumor is becoming molecularly more complex, which concurs with the increased clinical difficulty in treating patients who have developed resistance to first-line targeted therapy.

Abstract:

Purpose: The aim of this study was to investigate the effect of VEGF targeted therapy (sunitinib) on molecular intratumoral heterogeneity (ITH) in metastatic clear cell renal cancer (mccRCC).

Experimental design: Multiple tumor samples (n=187 samples) were taken from the primary renal tumors of mccRCC patients who were sunitinib treated (n=23, SuMR clinical trial) or untreated (n=23, SCOTRRCC study). ITH of pathological grade, DNA (aCGH), mRNA (Illumina Beadarray) and candidate proteins (reverse phase protein array) were evaluated using unsupervised and supervised analyses (driver mutations, hypoxia and stromal related genes). ITH was analysed using intratumoral protein variance distributions and distribution of individual patient aCGH and gene expression clustering.

Results: Tumor grade heterogeneity was greater in treated compared to untreated tumors (P=0.002). In unsupervised analysis, sunitinib therapy was not associated with increased ITH in DNA or mRNA. However, there was an increase in ITH for the driver mutation gene signature (DNA and mRNA) as well as increasing variability of protein expression with treatment ($p<0.05$). Despite this variability, significant chromosomal and transcript changes to key targets of sunitinib, such as VHL, PBRM1 and CAIX, occurred in the treated samples.

Conclusions: These findings suggest that sunitinib treatment has significant effects on the expression and ITH of key tumor and treatment specific genes/proteins in mccRCC. The results, based on primary tumor analysis, do not support the hypothesis that resistant clones are selected and predominate following targeted therapy.

Introduction

A number of targeted agents are available for the treatment of metastatic clear cell renal cell cancer (mccRCC), of which a VEGF tyrosine kinase inhibitor (TKI), sunitinib, is most prominent (1). Clinical benefit with sunitinib varies between mccRCC patients, however resistance usually develops within a year in all patients. Unlike some other tumors (2), the mechanism of TKI resistance in mccRCC is unclear.

Recent analysis of primary and metastatic RCC tissue showed significant DNA intratumoral heterogeneity (ITH), driving the hypothesis that a process of clonal evolution occurs within RCC (3,4). Theoretically the presence of ITH is relevant in the development of resistance to VEGF targeted therapy. It is hypothesised that one of two possible scenarios occurs in resistance to targeted therapy: (i) a single resistant clone, potentially present at baseline, predominates during resistance resulting in reduced ITH with therapy; or (ii) a multifactorial process of acquired polyclonal resistance occurs, in which there is an initial increase in ITH with the potential for development of multiple resistant clones (5).

To evaluate the effect of TKIs on ITH and provide further evidence regarding likely mechanisms of resistance to targeted therapy, multiregion tissue sampling and DNA, RNA, protein expression analysis was performed on a cohort of primary ccRCC tumors from sunitinib naïve and treated mccRCC patients to identify if: (i) molecular heterogeneity also occurred at a RNA and protein level; and (ii) a period of sunitinib treatment (18 weeks) exacerbated molecular heterogeneity. Ideally, to answer the latter question one would undertake multi-region tumor sampling both before and after the sunitinib treatment, but before nephrectomy. Such an experiment would not be ethical or permissible. As such, we used a comparator group in the form of patients with well-matched sunitinib naïve tumors. Sunitinib has specific molecular

targets and has an effect on stromal elements within the tumor (4,6). It is conceivable that whilst sunitinib has little effect on ITH of the whole genome it may have specific effects on drug targets and driver mutations. Also, sunitinib may have inconsistent effects on the ITH of different components of the tumor, e.g. increased ITH may be solely due to increased variability of host response to the drug in stromal elements (such as variable lymphocyte infiltration (4)), rather than direct changes to variability of tumor clones. As such, we hypothesised that sunitinib treatment results in an increase in ITH of treatment specific genes, due to treatment related pressure. Therefore, in addition to unsupervised analysis, supervised analysis was undertaken for ITH in genes associated with: (i) key driver mutations in renal cancer; (ii) stromal elements; and (iii) molecular (mainly hypoxia related) targets of sunitinib. Understanding the effect of therapy on ITH gives insight into mechanisms of drug resistance and facilitates future biomarker work and drug development.

Methods

Patients and samples

Adequate fresh frozen primary ccRCC tissue for analysis was obtained from the cytoreductive nephrectomy samples of 23 sunitinib naive mccRCC patients as part of the Scottish Collaboration On Translational Research into Renal Cell Cancer (SCOTRRCC) study (UK CRN ID: 12229). Fresh frozen primary tumor tissue was also obtained from 27 mccRCC patients treated with 3 cycles of sunitinib (18 weeks) followed by a cytoreductive nephrectomy after 2 weeks off sunitinib as part of the Upfront Sunitinib (SU011248) Therapy Followed by Surgery in Patients with Metastatic Renal Cancer: a Pilot Phase II Study (SuMR; ClinicalTrials.gov identifier: NCT01024205); 23 of these patients had adequate tissue for analysis. Investigations were approved by institutional review boards and written, informed consent was obtained from each patient

Tissue Mapping

Tissue was obtained from at least three spatially separate regions of the kidney tumor (more regions if the size of the tumor allowed). Tissue processing was then performed as previously described (7). Briefly, if required each piece of tumor tissue was mapped and divided into smaller pieces (~1cm^3) in preparation for lysate creation. A cryostat section was performed on each 1cm^3 piece of tissue to confirm the presence of viable ccRCC and for grading (low grade, high grade or mixed low/high grade) by 2 independent histopathologists (MO, DB). A minimum of four protein/DNA/RNA lysates were aimed for per patient, from each morphologically differing region within each tumor.

Nucleic acid/protein extraction from tissue

(i) Nucleic acid

DNA extraction from fresh frozen tissue was carried out using the DNeasy Blood and Tissue Kit (Qiagen, UK) according to the manufacturer's instructions. The only significant alternation to the standard protocol was the addition of a PBS washing step to remove OCT compound carried over from the process of producing cryostat sections. Samples were fragmented prior to proteinase K digestion using a Qiagen Tissue Lyser. aCGH hybridisation was carried out as described (8).

RNA extraction was carried out using miRNEasy Kit (Qiagen, UK) according the manufacturer's protocols. Amplification and analysis of the RNA was as previously described (9).

(ii) Protein

50-75mg of tissue was placed into 2ml tubes with 990µl of lysis buffer (50mM Tris–HCl (pH 7.5), 5mM EGTA (pH 8.5), 150mM NaCl) supplemented with aprotinin (10mg/mL), phosphatase inhibitor cocktail A (Sigma, UK), phosphatase inhibitor cocktail B (Sigma, UK) and a protease inhibitor cocktail (Roche, UK). A single 5mm steel ball was added to each tube and the samples were homogenised at 50Hz twice for 5 minutes using a TissueLyser (Qiagen, UK). 10µl of Triton X-100 was added to each sample before centrifuging at 13,000g for 30 min at 4°C after which supernatants were transferred to fresh microcentrifuge tubes. Total protein concentrations were determined by BCA assay (Sigma, UK) and normalised to 1mg/mL.

Array-based comparative genomic hybridisation

aCGH hybridisation and analysis was carried out as recently described (8) using Roche UK Nimblegen 12X135k whole-genome array. The CGH-segMNT module of NimbleScan was used for the analysis with a minimum segment length of five probes and an averaging window of 130kb. Nimblegen arrays were positionally annotated based upon hg19 genomic coordinates and log ratio data was pre-processed in R as previously described (10). Briefly, array data was normalised with print tip Loess from the limma package to produce normalised log ratios, filtered to remove outliers based upon a 1 MAD deviation of each probe from its immediate genomic neighbours and smoothed with a circular binary segmentation algorithm from the DNACopy package. Smoothed log ratios were then thresholded for gain/loss (±0.1) and amplification/deletion (±0.45) to identify contiguous copy number aberrations containing at least 15 consecutive probes. For clustering categorical aCGH states representing gain, loss, amplification and deletion were clustered based upon Euclidean distance using a Ward's algorithm using the segmented values from the whole genome in each case. aCGH data available via GEO (Accession number GSE67818).

VHL genotyping

VHL genotyping (East of Scotland Regional Molecular Genetics Service, Ninewells Hospital, Dundee, UK) included sequence analysis of exons 1-3 of the VHL gene to detect mutations in the coding region plus multiplex ligation-dependant probe amplification for large deletions.

Gene expression analysis

mRNA was amplified using the WT-Ovation FFPE System Version 2 (NuGEN, UK), purified using the Qiaquick PCR Purification Kit (Qiagen, UK), biotinylated using the Encore BiotinIL ModuleIL (NuGEN, UK), purified using minElute Reaction Cleanup Kit (Qiagen, UK) and quantified using a Bioanalyser 2100 with RNA 6000 Nano Kit (Agilent, UK). cRNA was then hybridised to Human HT-12v3 expression Beadarrays (Illumina, Cambridge, United Kingdom) according to the standard protocol for NuGEN amplified samples. Gene expression data was read and normalised with the lump package in R using variance stabilisation and robust spline normalisation. Illumina expression data was annotated based upon ensembl gene annotation (hg19, release 61). Processed data was filtered to remove probes flagged as undetected in more than 50% of the 192 samples analysed and probes with replicate gene identifiers were removed selecting those with the highest variance for each gene. For unsupervised clustering the most informative probes were selected as those with a median absolute deviation across the dataset of greater than 0.6 leaving an intrinsic dataset representing 1787 probes from unique genes. Filtered expression data was then clustered based upon Euclidean distance using a Ward's algorithm. Gene expression data available via GEO (Accession number GSE65615).

Supervised copy number variation (CNV) and gene expression analysis

Supervised analysis was performed in order to assess clustering of individual patient tumor DNA and mRNA samples and CNV or differential gene expression with respect to molecules of relevance in renal cell cancer: (a) key molecular targets of sunitinib and hypoxia related genes; (b) stromal associated genes (extracellular matrix, stromal remodelling, and adhesion molecules) were utilised as previously described (11); and (c) a driver mutation gene set which was derived

from those genes mutated in greater than 3% of the cases in the TCGA renal clear cell dataset. For ordered clustering treatment groups were ordered according to the number of copy number changes in each case from left to right in the aCGH figures and for the mean total expression of all the genes in the list in the expression heat maps.

Reverse phase protein arrays (RPPA)

RPPA samples protein levels were determined and slides spotted as described previously (7,12). Briefly, batch effects across the three slides per marker were mitigated using ComBat (13) and normalized (VSN (14)). 58 proteins making up key functional groups of proteins in RCC pathogenesis or sunitinib response were selected for study (tables S1&S2). There was no signal detected for three of the proteins (Ki67, FLT3 and phospho-Jak2), leaving 55 proteins for analysis (antibodies detailed in table S1).

Statistical analysis

As described previously, aCGH (15) and gene expression (10) cluster dendrograms were created and cut into 30 branches, those patients whose tissue samples all fell within the same branch were defined as clustered. Heterogeneity was assigned where an individual patient's samples were split between two or more clusters within the dendrogram.

Intratumoral protein variance was calculated separately for untreated and sunitinib treated patients in an ANOVA framework. Untreated and treated variance distributions combining data from all 55 proteins were compared by a Mann-Whitney test (MW). Intratumoral variances for individual proteins were compared by an F-test where assumptions of normality and homoscedasticity held, respectively assessed using the Lillefours and Fligner tests; false

discovery rate (FDR) correction was applied (16). Differential protein expression between untreated and treated patient samples was tested for each protein using a Student t-test where normality and homoscedasticity assumptions were met, otherwise MW was performed; FDR was applied over combined t-test and MW values (16).

The MW/t-test and chi-square test/Fisher's exact test were used to test differences in continuous variables and categorical variables between the 2 groups, respectively. Pearson's correlation coefficient was used to calculate correlation using non-parametric data. P-values of <0.05 were taken as significant and all P-values were two-tailed. SPSS version 21 (IBM Corporation, Armonk, NY) or the R package (version 2.11.1) was used for all statistical analyses.

Results

Patient demographics

Of the 50 patients included in this study there was adequate tissue for analysis from 46 patients. The characteristics and clinical outcomes of the two patient cohorts (sunitinib treated and untreated) are given in table 1; the two groups were comparable other than for tumor grade (see below). Multiple tissue samples were obtained for all patients (total=187 samples). The precise number of replicate samples for analysis from each patient was driven by the specific availability of tissue. Multiple protein lysates were obtained from 44 patients (median 4 regions, (range 2-10 regions)). Multiple DNA lysates were obtained from 42 patients (median 3 regions (range 2-5 regions)). Multiple RNA lysates were obtained from 36 patients (median 3 regions (range 2-8 regions)).

Morphological heterogeneity of sunitinib naive and treated mccRCC samples

Tumor grade was assessed in multiple regions from each tumor to assess ITH (table 1). A homogeneous grade (tumor contained either low or high grade, but not both grades) occurred in 26 (57.8%) samples while heterogeneous grading (tumors containing both low and high grade elements) occurred in 19 (42.2%). Significantly more treated tumors expressed morphological heterogeneity compared to untreated tumors (65.2% vs 18.2%; P=0.002).

Unsupervised aCGH analysis to assess global genetic instability and ITH

Comparison of aCGH results, from multiple DNA samples, taken from spatially different areas of each tumor showed variable intratumoral clustering (table 2). In sunitinib naive tumors, 23/67

(34.3%) patient DNA samples clustered compared with DNA from 25/61 (41.0%) sunitinib treated samples (P=0.44, fig. 1A), suggesting substantial underlying genetic ITH in mccRCC primary tumors which was not significantly altered by sunitinib. Although the extent of ITH did not alter with sunitinib, there were significantly greater levels of chromosomal gains, amplifications and deletions in treated compared with untreated samples ($p<0.03$) (fig. 1B).

Unsupervised gene expression analysis to determine global transcriptomic ITH

Hierarchical clustering of gene expression results from multiple RNA samples from each tumor showed that there was intratumor clustering in 24/36 patients (fig. 1C & table 2). There was a greater proportion of patients whose RNA clustered compared with DNA clustering (table 2) 24/36 (67%) vs 17/42 (40.5%) patients respectively (p=0.025). As with the DNA analysis, there was comparable intratumoral clustering of untreated patient RNA samples, 26/43 (60.5%) RNA samples, compared with, 48/73 (65.8%) RNA samples from treated patients, P=0.69.

Correlation of sample clustering for DNA and gene expression

There were 33 patients with clustering results available for both DNA and RNA. Eight patients (24.2%) had both DNA and RNA samples which clustered, 17 patients (51.5%) had either RNA or DNA which clustered and in 8 patients (24.2%) neither RNA nor DNA was determined to have clustered. Clustering of either DNA or RNA made clustering in the other nucleic acid more likely (P=0.015).

Effect of sunitinib treatment on intratumor protein heterogeneity and protein expression

Intratumoral variance in expression of candidate proteins, measured using RPPA, was marked in untreated patient samples (fig. 2A). But protein variance was even higher in the sunitinib treated samples compared to the untreated samples (40/55, P=0.001; fig. 2B). Despite exacerbation of protein variance by sunitinib, there were significant differences in median expression of 30 of the 55 proteins evaluated (table S2). There was no correlation of the effect of sunitinib on differential RNA and protein expression (fig. S1). Consistent, significant changes for both mRNA and protein were only seen for 1 of the 55 proteins evaluated (Cyclin D1).

Supervised aCGH and gene expression analysis to assess ITH of relevant pathways

Three key groups of genes, relevant in renal cancer pathogenesis and TKI treatment were assessed to observe for ITH and to assess which tumor component may be driving protein ITH following sunitinib therapy. Key driver mutations, hypoxia associated genes and stroma related genes were assessed for aCGH derived CNVs (table 2 & fig. S2) and gene expression analysis (table 2 & fig. S2). Considering CNVs, there was a significant reduction in individual patient sample clustering of driver mutation (P=0.032) and hypoxia genes (P<0.001) in treated patients, suggesting increased ITH.

For gene expression analysis clustering, driver mutation genes, hypoxia and stroma associated genes had less clustering in treated samples than untreated patient samples (table 2 & fig. S2); this reduction in clustering was significant for driver mutation (p=0.006) and stroma associated genes (P=0.016) but not hypoxia genes (P=0.29).

Differential copy number variation and gene expression between untreated and treated patients

Comparison of untreated and treated DNA samples revealed the significant gains or losses in the region of the following key genes (fig. 3). In the treated samples there were gains of VEGFR3 and PDGFRβ and losses for VCAM1, HIF1α, CAIX, mTOR, BAP1, PBRM1, SETD2 and VHL. Of note, no significant CNVs were seen to VEGFR2 (KDR).

Similarly, gene expression profiles of untreated and treated patient tumor RNA samples were compared (fig. 4). Vimentin, clusterin, PDGFα, PDGFβ, VEGFA, VEGFR2 (KDR), HIF1α and CAIX all had significantly greater expression in treated tumor samples. PBRM1, KDM5C, VHL and PDGFC had significantly lower levels of expression in the treated samples.

Discussion

Initially we showed that primary ccRCC tissue from patients treated with sunitinib expressed greater morphological heterogeneity (of tumor grade) compared to tumors from untreated patients. This was intriguing and, in view of the similar characteristics of the patient cohorts, was postulated to be treatment rather than patient related. These findings built on our previous findings from paired, sequential biopsy and nephrectomy samples which showed that sunitinib therapy was associated with increased tumor grade, lymphocyte infiltration and proliferation (Ki-67 expression) (4). This increase in pathological ITH prompted further investigation at the molecular level to determine if sunitinib treatment was associated with dynamic molecular changes resulting in a more aggressive tumor phenotype. There has been extensive work on DNA heterogeneity at a single time point, resulting in the hypothesis of specific somatic mutations, following a pattern of clonal evolution (3). In the work presented above it was hypothesised that sunitinib treatment results in an increase in ITH of treatment specific genes, due to treatment related pressure; such clonal divergence may facilitate the evolution of resistant phenotypes.

In order to test the hypothesis, we performed chromosomal, RNA and protein based analyses. Results identified ITH at every molecular level investigated, in both treated and untreated samples. A comparison of mRNA and DNA results showed less ITH at a transcript level, suggesting ITH was predominantly genetic. Overall, approximately only half of multiple DNA or mRNA samples from individual tumors clustered together demonstrating the extent of the ITH. As has been previously demonstrated (17), there was remarkable inconsistency regarding mRNA and protein expression in both treated and untreated samples. Cyclin D1 was the only molecule for which a mRNA-protein correlation was found, potentially suggesting it for

future multi-level molecular analysis. Despite this, there was a positive correlation between tumors with both DNA clustering and mRNA clustering, suggesting some consistency within tumors at different levels of molecular analysis. Therefore the process of ITH was not purely random or molecular technique specific, but individual tumors appeared to have different degrees of ITH, which was consistent across DNA and mRNA.

The effect of VEGF treatment on ITH at a molecular level is unknown in renal cancer. Indeed, to our knowledge there is an absence in the literature for any tumor type. Unsupervised analysis did not reveal any significant effect of sunitinib therapy on ITH at a chromosomal or mRNA level. This finding may have been expected as sunitinib has specific effects and is therefore unlikely to affect the whole genome significantly. However, results from supervised analyses showed a consistent increase in ITH for both DNA and mRNA of the renal cancer driver mutation genes. The degree of DNA and RNA ITH of stromal and hypoxia related genes following sunitinib therapy was inconsistent. The consistent increase in ITH in the driver mutations and the lack of consistent results in the stromal genes suggests that the findings are, at least in part, tumor related rather than purely stromal related reactions to therapy. Our results suggest dynamic changes to heterogeneity in the tumor, vascular and stromal components may be distinct with sunitinib. Whether changes to specific genetic alterations/expression are due to direct effects of treatment on the tumor or indirect effects on the tumor/stroma ratio remain uncertain. These findings were supported by protein expression results where an increase in ITH was observed for selected tumor specific proteins. It is conceivable that sunitinib causes diversification of protein expression within tumors as a reaction to treatment associated factors such as hypoxia, as postulated previously for other tumors (18).

The relatively short period of targeted treatment (18 weeks), consistent time between cessation of sunitinib and nephrectomy and the significant changes to selected relevant targets indicate that the exacerbated ITH in treated samples is likely to be treatment related rather than simply time related.

These results allow the development of further hypotheses regarding the mechanism of acquired resistant to VEGF targeted therapy in mccRCC. The findings presented here do not support the hypothesis that a single resistant clone predominates from a number of clones after treatment commences, as treatment was associated with more rather than less ITH. As such, it can be speculated that there may be an expansion of clones, facilitating the development of resistant clones, that is polyclonal drug resistance (5). Further work using circulating samples or multiple biopsies at multiple time points throughout drug treatment would be required to prove the development of polyclonal drug resistance and allow the development of clinically relevant strategies to overcome drug resistance

These findings may be relevant in optimizing the timing of immune checkpoint inhibitors in metastatic RCC. These therapies may work best in tumors with a high mutational burden (19). Therefore starting checkpoint inhibitor therapy after a short period of VEGF targeted therapy, when mutational burden may be higher is attractive. This approach should be considered for future clinical trials.

The final finding was that despite ITH, consistent chromosomal, RNA and protein changes to the targets of sunitinib were seen with treatment, in keeping with our previous findings regarding consistent changes in CAIX protein expression following sunitinib treatment (12). Notable CNVs identified were losses of the renal cancer driver genes SETD2, BAP1, VHL and PBRM1 (latter two genes also had a significantly lower level of gene expression) following

sunitinib therapy (20). BAP1 and PBRM1 loss have previously been shown to be associated with a poor prognosis (21). It should be noted that, together with greater levels of 3p loss in the treated patient cohort, enrichment of the 3p tumor suppressors maybe due to intrinsic differences in the unmatched patient cohorts rather than treatment; although this is thought to be unlikely due to the comparable VHL mutation rate of 78% in the untreated patients and 65% in the treated patients. Overall, these genetic alterations suggests that sunitinib is having direct effects on the tumor and further supports the hypothesis that the changes seen with sunitinib are not purely a time related phenomena.

We recognize the limitations of this study. Firstly, although the characteristics of the two groups were similar, the treated and untreated samples frozen were not matched from the same patients. However, obtaining multiple frozen samples from nephrectomy patients is challenging, requiring close interaction between urologists and pathologists (22); the multi-region sample set described here is to our knowledge the largest available. The ideal validation set of matched pre- and post-treatment multiregion sampled tumors is not feasible or ethical and a similar validation cohort to ours was unavailable. However, the multilevel analysis performed in this study, with all analyses confirming increasing ITH with treatment, acts as internal validation of the conclusions. Secondly, there was a two-week break between sunitinib completion and nephrectomy, which may have influenced the results in the treated patients. Finally, sunitinib was given for a fixed period and responses to sunitinib were variable. Therefore treated samples may have been at different stages of clonal evolution. Finally, there is a justified concern that identification of specific tumor related results might be contaminated by treatment-induced changes to the proportion of the stromal component within the tumor. The supervised analysis presented in this

study attempted to address this concern; however, this is a consideration when interpreting the data presented.

The results of this study demonstrate a more complex tumor appears to be developing following sunitinib therapy. The resulting tumor is likely to be difficult to target successfully using a 'one size fits all approach' as is currently standard of care in VEGF-targeted therapy resistant disease. These findings may in part explain why treatment in relapsed disease is particularly challenging (23).

Acknowledgments: Thanks to Wellcome Trust Clinical Research Facility Genetics Core, Edinburgh for assistance with undertaking gene expression analysis and Morad Ansari for performing aCGH.

References

1. Motzer RJ, Hutson TE, Tomczak P, Michaelson MD, Bukowski RM, Oudard S, et al. Overall survival and updated results for sunitinib compared with interferon alfa in patients with metastatic renal cell carcinoma. J Clin Oncol Off J Am Soc Clin Oncol. 2009;27:3584–90.

2. Wagle N, Van Allen EM, Treacy DJ, Frederick DT, Cooper ZA, Taylor-Weiner A, et al. MAP Kinase Pathway Alterations in BRAF-Mutant Melanoma Patients with Acquired Resistance to Combined RAF/MEK Inhibition. Cancer Discov. 2013;

3. Gerlinger M, Rowan AJ, Horswell S, Larkin J, Endesfelder D, Gronroos E, et al. Intratumor heterogeneity and branched evolution revealed by multiregion sequencing. N Engl J Med. 2012;366:883–92.

4. Sharpe K, Stewart GD, Mackay A, Van Neste C, Rofe C, Berney D, et al. The effect of VEGF-targeted therapy on biomarker expression in sequential tissue from patients with metastatic clear cell renal cancer. Clin Cancer Res Off J Am Assoc Cancer Res. 2013;19:6924–34.

5. Burrell RA, Swanton C. Tumour heterogeneity and the evolution of polyclonal drug resistance. Mol Oncol. 2014;

6. Huang D, Ding Y, Li Y, Luo W-M, Zhang Z-F, Snider J, et al. Sunitinib acts primarily on tumor endothelium rather than tumor cells to inhibit the growth of renal cell carcinoma. Cancer Res. 2010;70:1053–62.

7. O'Mahony FC, Nanda J, Laird A, Mullen P, Caldwell H, Overton IM, et al. The use of reverse phase protein arrays (RPPA) to explore protein expression variation within individual renal cell cancers. J Vis Exp JoVE. 2013;

8. Gerth-Kahlert C, Williamson K, Ansari M, Rainger JK, Hingst V, Zimmermann T, et al. Clinical and mutation analysis of 51 probands with anophthalmia and/or severe microphthalmia from a single center. Mol Genet Genomic Med. 2013;1:15–31.

9. Turnbull AK, Kitchen RR, Larionov AA, Renshaw L, Dixon JM, Sims AH. Direct integration of intensity-level data from Affymetrix and Illumina microarrays improves statistical power for robust reanalysis. BMC Med Genomics. 2012;5:35.

10. Natrajan R, Weigelt B, Mackay A, Geyer FC, Grigoriadis A, Tan DSP, et al. An integrative genomic and transcriptomic analysis reveals molecular pathways and networks regulated by copy number aberrations in basal-like, HER2 and luminal cancers. Breast Cancer Res Treat. 2010;121:575–89.

11. Turnbull AK, Arthur L, Renshaw L, Larionov AA, Kay C, Dunbier AK, et al. Accurate prediction and validation of response to endocrine therapy in breast cancer. J Clin Oncol. 2015;In press.

12. Stewart GD, O'Mahony FC, Laird A, Rashid S, Martin SA, Eory L, et al. Carbonic Anhydrase 9 Expression Increases with Vascular Endothelial Growth Factor–Targeted Therapy and Is Predictive of Outcome in Metastatic Clear Cell Renal Cancer. Eur Urol. 2014;66:956–63.

13. Johnson WE, Li C, Rabinovic A. Adjusting batch effects in microarray expression data using empirical Bayes methods. Biostat Oxf Engl. 2007;8:118–27.

14. Neeley ES, Kornblau SM, Coombes KR, Baggerly KA. Variable slope normalization of reverse phase protein arrays. Bioinformatics. 2009;25:1384–9.

15. Natrajan R, Lambros MB, Rodríguez-Pinilla SM, Moreno-Bueno G, Tan DSP, Marchió C, et al. Tiling Path Genomic Profiling of Grade 3 Invasive Ductal Breast Cancers. Clin Cancer Res. 2009;15:2711–22.

16. Benjamini Y, Hochberg Y. Controlling the False Discovery Rate: A Practical and Powerful Approach to Multiple Testing. J R Stat Soc Ser B Methodol. 1995;57:289–300.

17. Maier T, Güell M, Serrano L. Correlation of mRNA and protein in complex biological samples. FEBS Lett. 2009;583:3966–73.

18. Gillies RJ, Verduzco D, Gatenby RA. Evolutionary dynamics of carcinogenesis and why targeted therapy does not work. Nat Rev Cancer. 2012;12:487–93.

19. Snyder A, Makarov V, Merghoub T, Yuan J, Zaretsky JM, Desrichard A, et al. Genetic basis for clinical response to CTLA-4 blockade in melanoma. N Engl J Med. 2014;371:2189–99.

20. Brugarolas J. Molecular genetics of clear-cell renal cell carcinoma. J Clin Oncol Off J Am Soc Clin Oncol. 2014;32:1968–76.

21. Kapur P, Peña-Llopis S, Christie A, Zhrebker L, Pavía-Jiménez A, Rathmell WK, et al. Effects on survival of BAP1 and PBRM1 mutations in sporadic clear-cell renal-cell carcinoma: a retrospective analysis with independent validation. Lancet Oncol. 2013;14:159–67.

22. Stewart GD, Harrison DJ, Swanton C, Lewis R, Bliss J, Larkin J, et al. Multidisciplinary urological engagement in translational renal cancer research. BJU Int. 2014;114:474–5.

23. Motzer RJ, Escudier B, Oudard S, Hutson TE, Porta C, Bracarda S, et al. Efficacy of everolimus in advanced renal cell carcinoma: a double-blind, randomised, placebo-controlled phase III trial. Lancet. 2008;372:449–56.

Figure legends:

Fig. 1. Unsupervised aCGH and gene expression clustering results. (A) Heatmap demonstrating clustering of aCGH profiles of sunitinib naive and treated samples. Categorical aCGH states (i.e. gains, losses, and amplifications) were used for clustering, employing Ward's clustering algorithm based upon Euclidean distance. No significant difference in aCGH clustering was seen between treated and untreated patients (P=0.44; Fisher's test). **(B)** Comparisons of the number of aCGH aberrations in treated and untreated samples showed significantly more copy number gains, amplifications and deletions in treated patients than in untreated patients (t-test). **(C)** Heatmap demonstrating unsupervised clustering of gene expression profiles of sunitinib naive and treated samples. Filtered gene expression data was clustered based upon Euclidean distance using a Ward's algorithm. There were no significant difference in sample clustering between treated and untreated patients (P=0.69; Fisher's test). Heatmap is a representation of all probes, created using clusters containing treatment related genes and those driving the dendrogram.

Fig. 2. Protein results for sunitinib naive and treated samples. (A) Histogram demonstrating the intratumoral variance for each of the 55 proteins analysed with RPPA in sunitinib naive patients. **(B)** $\log_2$ within tumor variance ratio of sunitinib naive and treated samples. The number of proteins analysed for which the median intratumoral variance is greater in the sunitinib naive group (n=15); greater in the sunitinib treated group (n=40). There are significantly more proteins with higher median variance in the treated group than the untreated group (P=0.001, binomial-test). Proteins with variance below zero on y-axis are greater for the untreated primary tumor, those above the y-axis zero were greater in the treated primary tumor. Table S2 details the differential protein expression seen following sunitinib therapy.

Fig. 3. Supervised analysis of driver mutation, hypoxia and stromal molecules copy number variation between untreated and treated patients. Heat maps **(A)** driver mutations, **(B)** hypoxia and **(C)** stroma plotting gains/amplifications (red) and losses/deletions (blue) in corresponding gene regions. The right-hand bar represents the lod score (-log10) of the adjusted P-value (Fisher's test), dashed line represents P=0.05, bars are colored when significant (red, significant gain in treated patient samples; blue, significant loss in treated patient samples). The genes regions are ordered according by level of significance.

Fig. 4. Supervised analysis of driver mutation, hypoxia and stromal molecules gene expression between untreated and treated patients. Heat maps for gene expression levels of **(A)** driver mutations, **(B)** hypoxia and **(C)** stromal related genes. The right-hand bar represents the lod score (-log10) of the adjusted P-value (t-test), dashed line represents P=0.05, bars are colored when significant (red, greater expression in treated patient samples; blue, lower expression in treated patient samples). The genes are ordered according to the level of significance.

Table 1. Patient demographics, pathology details and clinical outcomes of patients donating tumor samples to this study.

Cohort	Total	Sunitinib naive	Sunitinib treated
Number of patients	46	23	23
Age, median (IQR) [a]	65.3 (59.0-72.9)	67.5 (59.2-72.9)	63.0 (56.0-73.0)
Male gender[a]	30 (65.2%)	14 (60.9%)	16 (69.6%)
Fuhrman grade[b]**:**			
1	0	0	0
2	14 (30.4%)	4 (17.4%)	10 (43.5%)
3	23 (50.0%)	11 (47.8%)	12 (52.2%)
4	9 (19.6%)	8 (34.8%)	1 (4.3%)
Stage[a]**:**			
T1	1 (2.2%)	0	1 (4.3%)
T2	6 (13.0%)	2 (8.7%)	4 (17.4%)
T3	33 (71.7%)	20 (87.0%)	13 (56.5%)
T4	6 (13.0%)	1 (4.3%)	5 (21.7%)
Grade[c,d]**:**			
Single	26 (57.8%)	18 (81.8%)	8 (34.8%)
Multiple	19 (42.2%)	4 (18.2%)	15 (65.2%)
Multiregion sampling[a]**:**			
Protein	44 (95.7%)	22 (95.7%)	22 (95.7%)
RNA	36 (78.3%)	18 (78.3%)	18 (78.3%)
DNA	42 (91.3%)	21 (91.3%)	21 (91.3%)
VHL status[a]**:**			
Mutation	33 (71.7%)	18 (78.3%)	15 (65.2%)
Wild type	13 (28.3%)	5 (21.7%)	8 (34.8%)
Number of metastatic sites[a]**:**			
1	22 (47.8%)	14 (60.9%)	8 (34.8%)
2	18 (39.1%)	7 (30.4%)	11 (47.8%)
3	6 (13.0%)	2 (8.7%)	4 (17.4%)
Heng classification[a]**:**			
Intermediate	25 (54.3%)	14 (60.9%)	11 (47.8%)
Poor	19 (41.3%)	7 (30.4%)	12 (52.2%)
Missing data	2 (4.3%)	2 (8.7%)	0
1st line TKI[e]	N/A	12 (52.2%)	N/A
Median overall survival, months (IQR)[a]	15.9 (9.0-25.9)	12.2 (6.7-19.4)	23.0 (13.6-30.0)

IQR=interquartile range
N/A=not applicable
P-values comparing sunitinib naive and sunitinib treated patients: [a]P>0.05; [b]P=0.02; [c]P=0.002
[d]1 sunitinib naive patient had inadequate tissue for grade analysis but enough tissue for multiregion sampling for RNA analysis only. Therefore denominator is 45 samples in total, 22 for sunitinib naïve patients and 23 for sunitinib treated patients.
[e]number of sunitinib naive patients who had post-nephrectomy TKIs.

Table 2. Details of individual patient clustering of DNA copy number variation and RNA expression. Black shaded boxed denote clustering for the indicated analysis for multiple samples from an individual patient.

DNA Copy Number Variation Clustering						
	PATIENT	NUMBER OF DNA SAMPLES PER PATIENT	UNSUPERVISED	STROMAL GENES	DRIVER MUTATION GENES	HYPOXIA GENES
Untreated	BB070193	3				
	BB090363	2				
	BB090175	4				
	BB100186	3		■		
	BB100333	3				
	BB100486	3	■	■	■	
	RN000010	4				■
	RN000003	2	■		■	■
	RN000006	3	■		■	■
	RN000027	3				■
	RN000028	5				■
	RN000035	3				
	RN000060	3	■			
	RN000065	3	■			
	RN000086	3	■		■	■
	RN000095	3				■
	RN000147	4				
	RN000160	3			■	■
	RN000173	3	■	■	■	■
	RN000184	4				
	RN000193	3	■		■	■
Samples clustering			23/67 (34.3%)	9/67 (13.4%)	20/67 (29.9%)	32/67 (56.1%)
Treated	SU01	3				
	SU04	3	■			
	SU05	3				
	SU06	3	■	■	■	■
	SU09	3				
	SU11	3				
	SU13	3				
	SU16	3				
	SU19	3				
	SU22	3				
	SU23	3				
	SU25	3	■			
	SU26	3	■			
	SU32	3	■	■		
	SU36	3	■			
	SU39	3	■	■	■	

	SU41	3				
	SU46	3				
	SU48	3				
	SU49	2				
	SU54	2				
Samples clustering			25/61 (41.0%)	13/61 (21.3%)	8/61 (13.1%)	5/61 (8.2%)
P-value (untreated vs. treated; Fisher's test)			0.44	0.25	0.032	5.465e-07

Gene Expression Clustering

	PATIENT	NUMBER OF RNA SAMPLES PER PATIENT	UNSUPERVISED	STROMAL GENES	DRIVER MUTATION GENES	HYPOXIA GENES
Untreated	BB070193	2				
	BB090363	3				
	BB090175	3				
	BB100186	2				
	BB100322	3				
	BB100333	3				
	BB100486	2				
	RN000010	2				
	RN000003	2				
	RN000006	2				
	RN000026	2				
	RN000027	2				
	RN000028	2				
	RN000035	2				
	RN000065	3				
	RN000160	2				
	RN000173	3				
	RN000184	3				
Samples clustering			26/43 (60.5%)	21/43 (48.9%)	8/43 (18.6)	15/43 (34.9%)
Treated	SU01	8				
	SU04	4				
	SU05	2				
	SU09	3				
	SU11	8				
	SU16	2				
	SU17	5				
	SU19	4				
	SU22	7				
	SU23	4				
	SU25	4				
	SU26	5				
	SU32	2				
	SU39	3				
	SU41	2				
	SU46	4				

	SU48	4	[redacted]			
	SU49	2				[redacted]
Samples clustering			48/73 (65.8%)	19/73 (26.0%)	0/73 (0%)	18/73 (24.7%)
P-value (untreated vs. treated; Fisher's test)			0.69	0.016	0.006	0.29

Figure 1

Author Manuscript Published OnlineFirst on May 26, 2015; DOI: 10.1158/1078-0432.CCR-15-0207

Figure 2

a

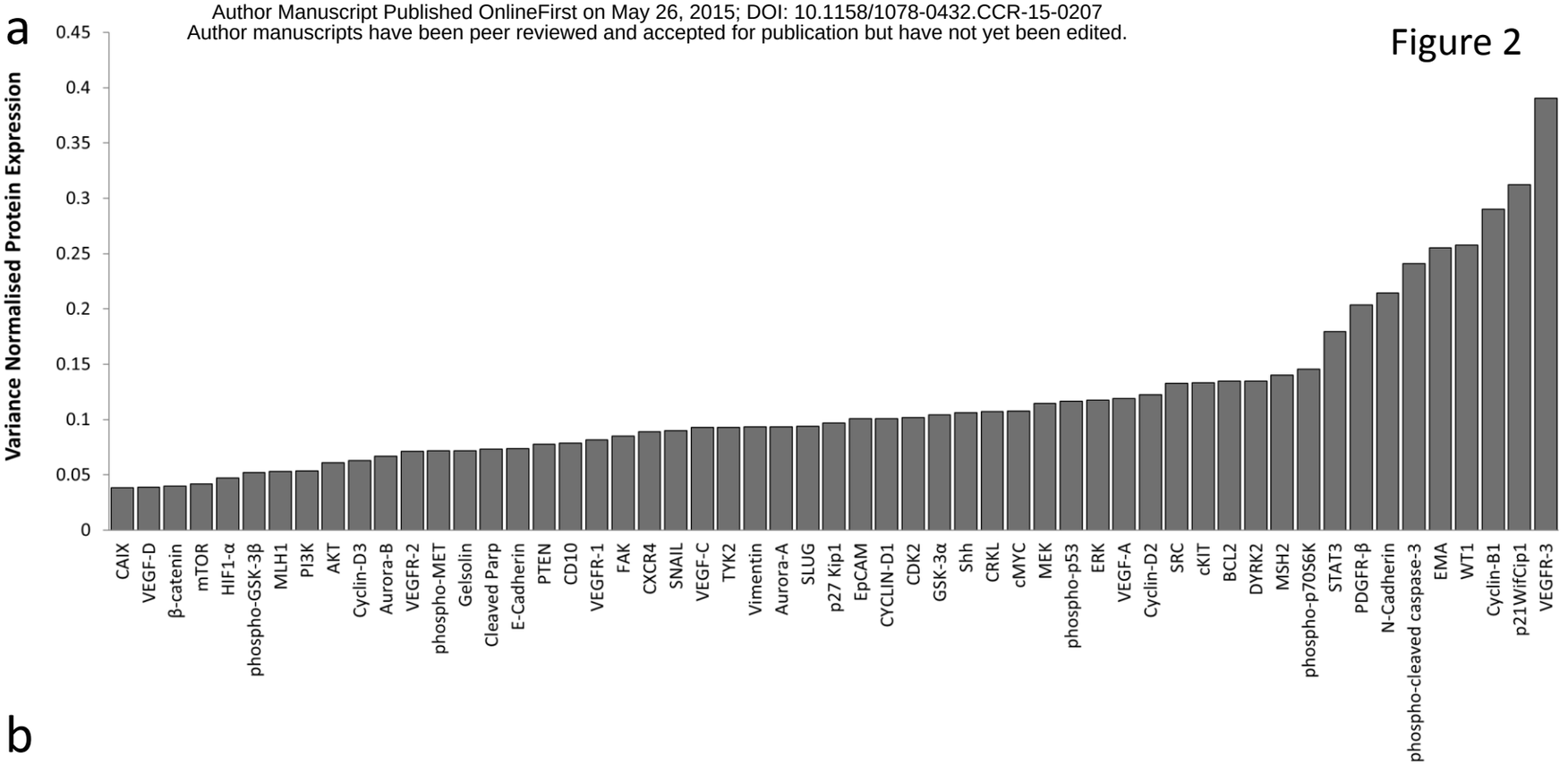

b

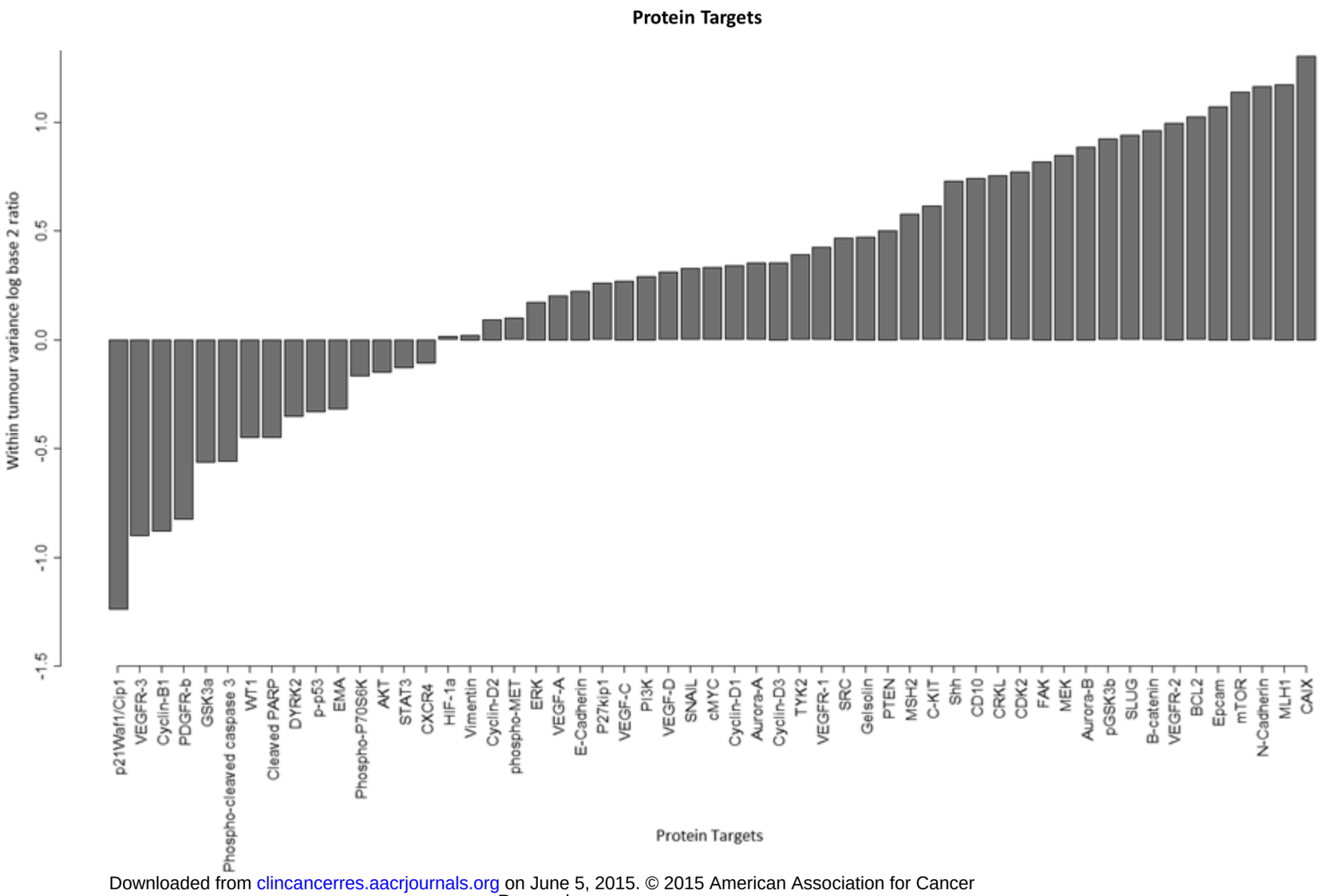

Figure 3

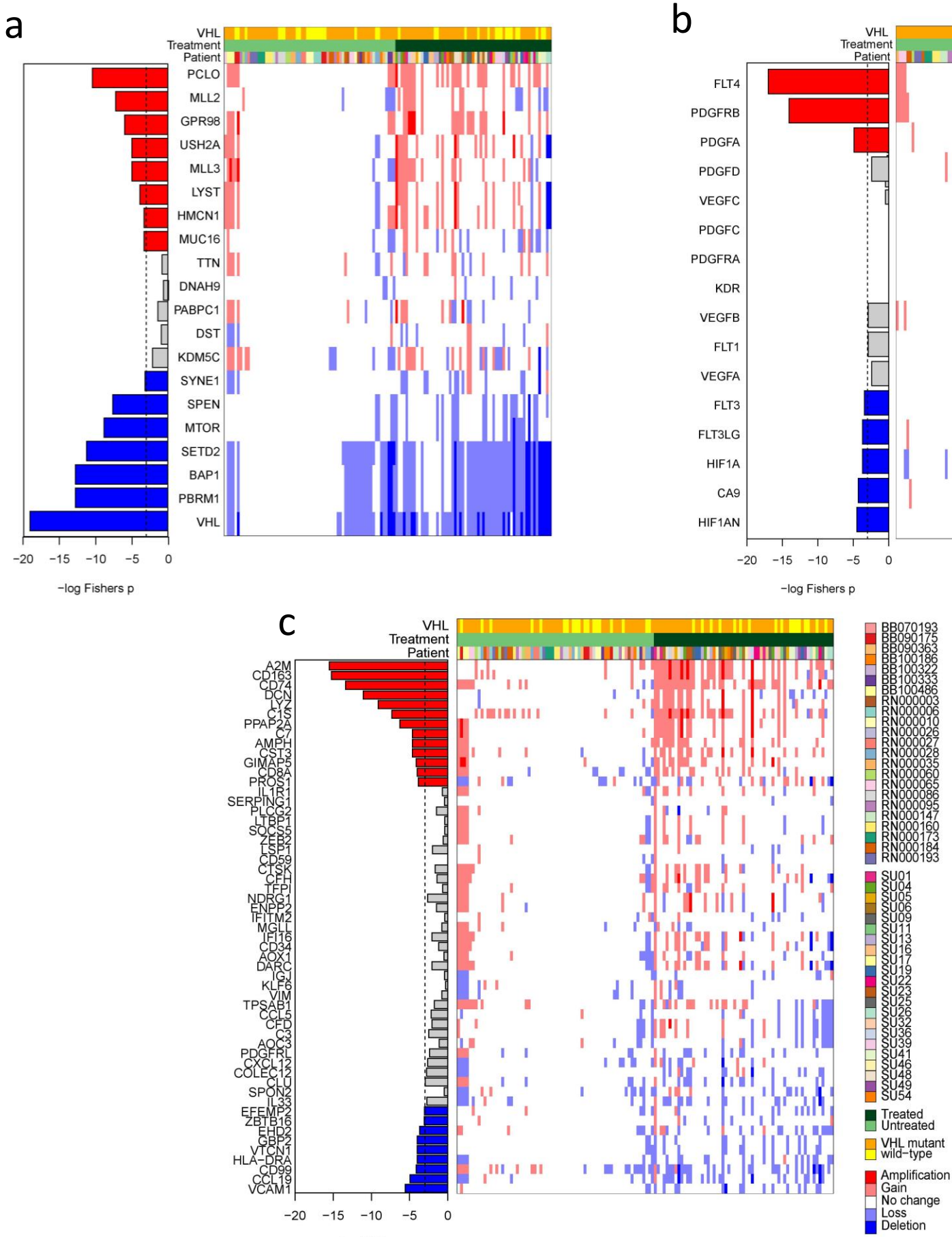

a

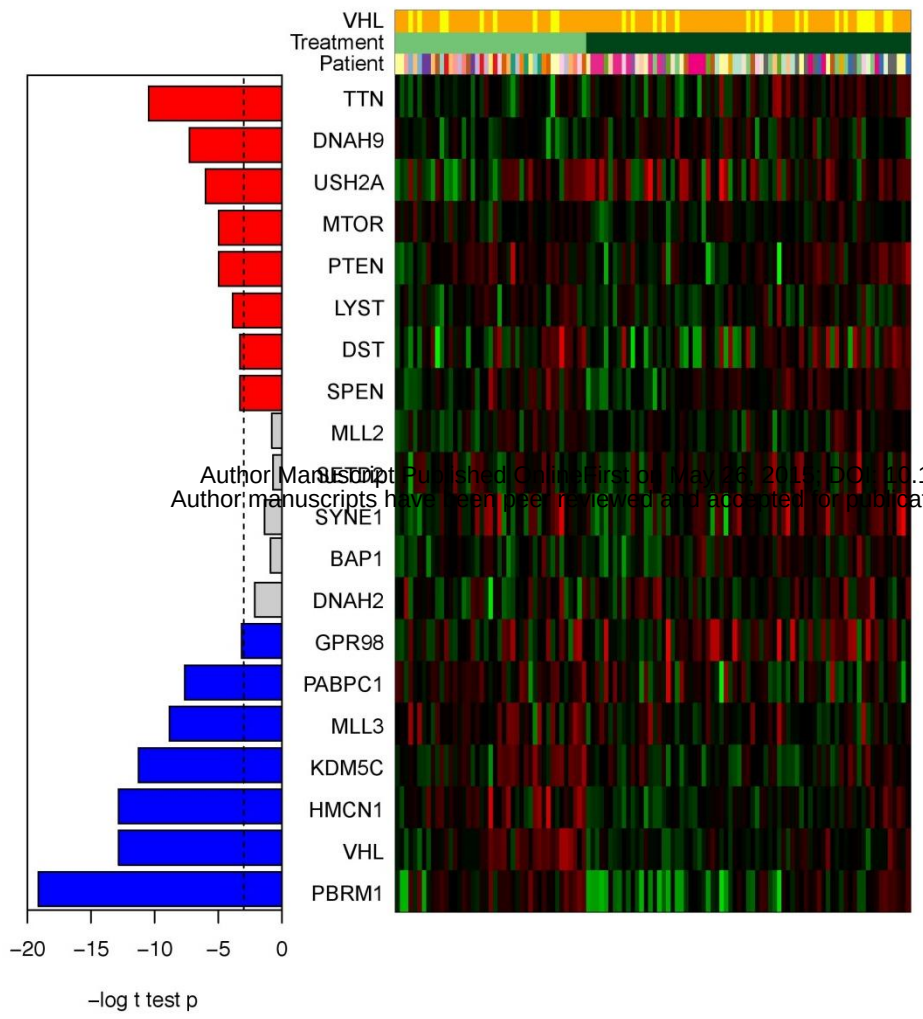

b

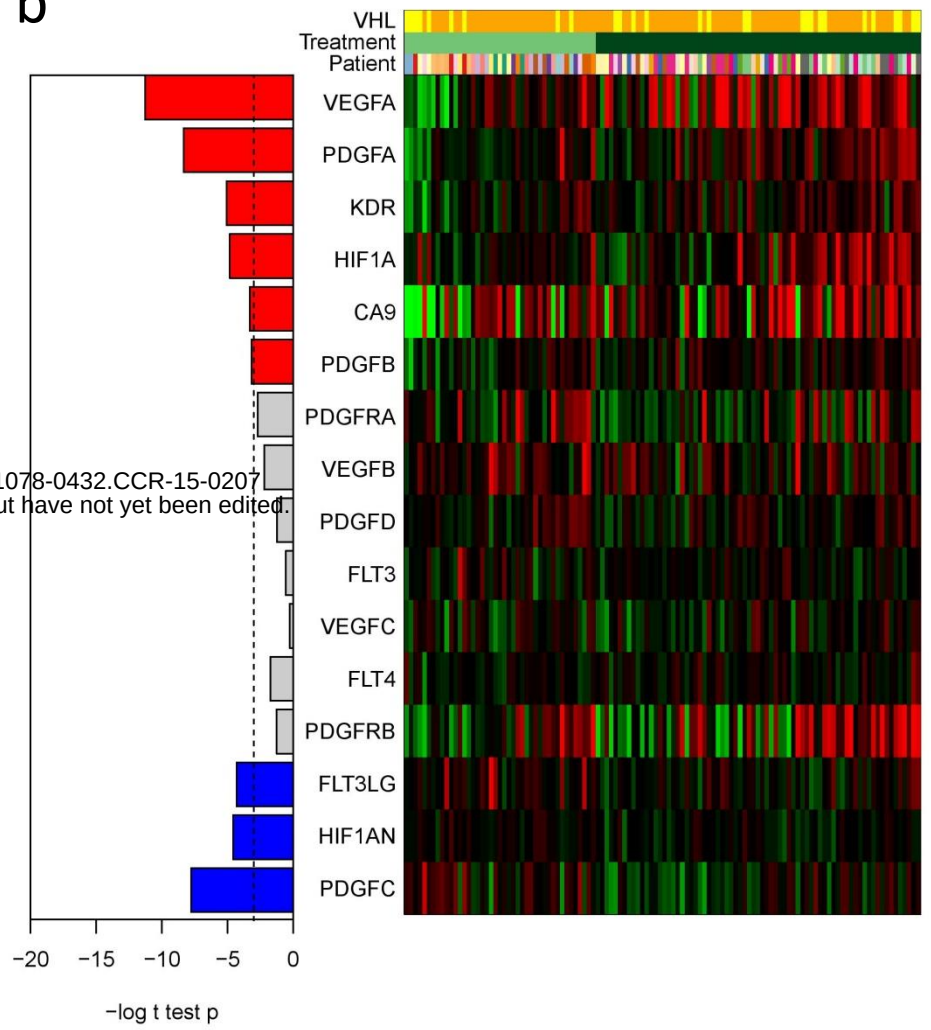

c

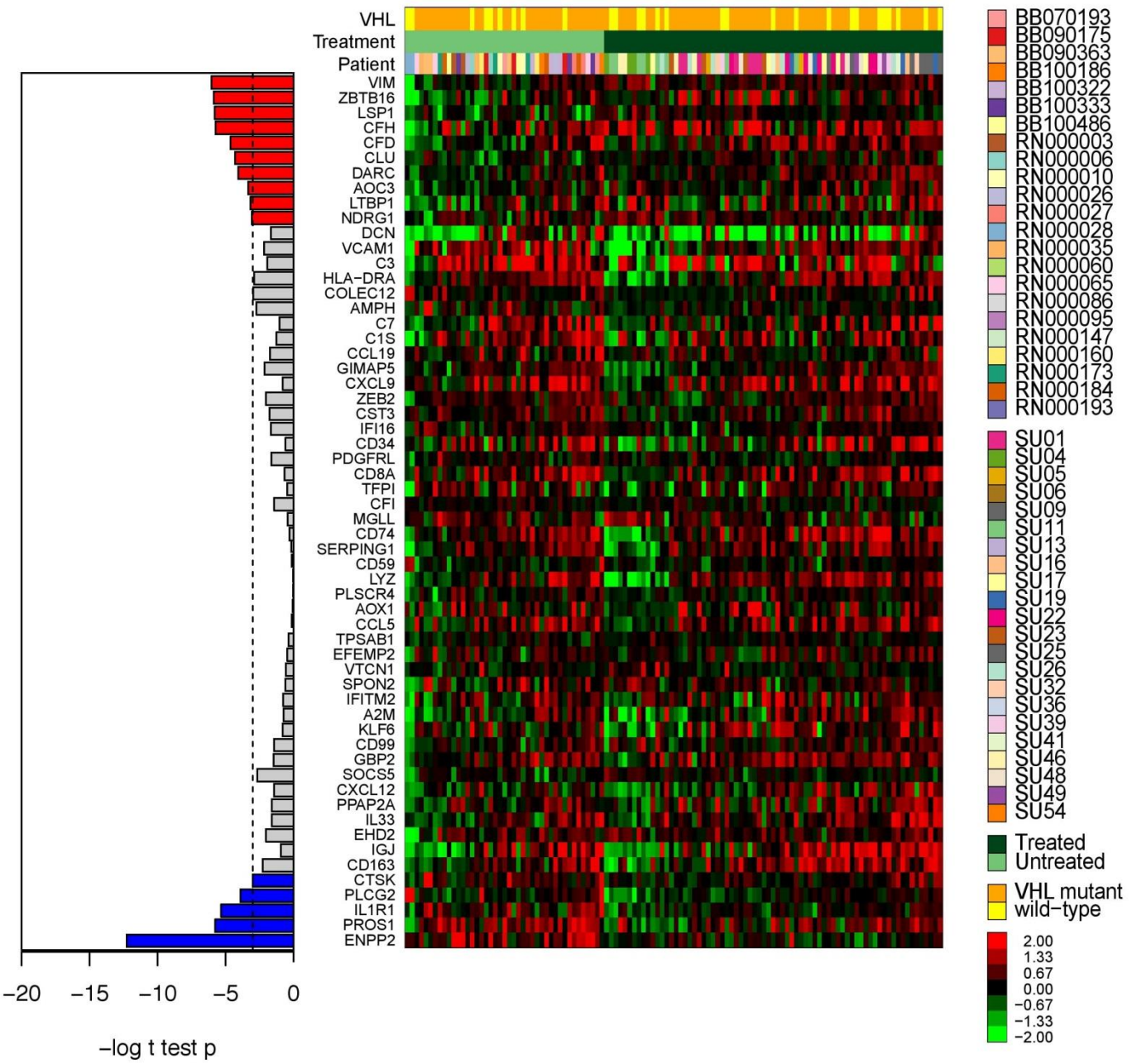

AACR American Association for Cancer Research

Clinical Cancer Research

Sunitinib treatment exacerbates intratumoral heterogeneity in metastatic renal cancer

Grant D Stewart, Fiach O'Mahony, Alexander Laird, et al.

Clin Cancer Res Published OnlineFirst May 26, 2015.